

Technical Note SNMREC-TN-12-062

March, 2012

Subsurface Mooring Stability in the Presence of Vertical Shear

Howard P. Hanson

Summary: Observations reveal significant vertical shear in the Florida Current that can occur on the scale of turbine rotors and that can reverse. Because ocean current turbines in the Florida Current will require anchored moorings, the dynamics of the moored systems in the presence of shear become a factor in design and deployment. Here, a simple analysis shows that the case of negative shear (slow current near the surface) is dynamically unstable for moored turbine systems.



Southeast National Marine Renewable Energy Center

College of Engineering and Computer Science / Florida Atlantic University

Page intentionally blank

Subsurface Mooring Stability in the Presence of Vertical Shear

Howard P. Hanson, SNMREC/FAU

Technologies for recovering power from open-ocean currents, such as the Florida Current in the Atlantic Ocean offshore southeast Florida, have much in common with technologies for power recovery from tidal flows. A critical difference, however, is the water depth. Tidal channels are typically tens of meters deep; the Florida Current, on the other hand, has its maximum current speeds near the surface in hundreds of meters of water. Thus, while tidal technologies can rely on bottom-mounted systems—the metaphor of an underwater wind turbine is quite reasonable here—in the open ocean other approaches are required.

Deep water locations—and there is no strict definition of “deep” in this context—generally preclude the use of masts or bases for deployment of OCTs. For one thing, deep water makes masts impractical; for another, open-ocean currents tend to be strongest near the surface.

In deep water, OCTs will require moorings whose anchors can provide sufficient holding strength and whose overall design can provide stability against variations in the current. Because the current is known to be subject to variations in both speed and direction as functions of both time and height above the bottom (e.g., Fig. 1), it is useful to examine the stability of a simple mooring/OCT system in the presence of vertical shear.

Consider the force diagram shown in Fig. 2. The current, flowing from left to right, induces a horizontal drag force **D** on the OCT, which also is subject to a net upward buoyancy force **B**. The vector sum of these two forces is balanced, in steady state, by the tension force **M** on the mooring rode (*i.e.*, the anchor line).



Figure 1: Current speed as a function of depth in the Florida Current 16 km offshore Dania Beach. The stippled area at the top denotes a shipping-lane depth zone, and the symbol represents (to scale) a 40-m diameter system deployed at 70 m. Note that the sign of the vertical shear in this layer is different for the two profiles.

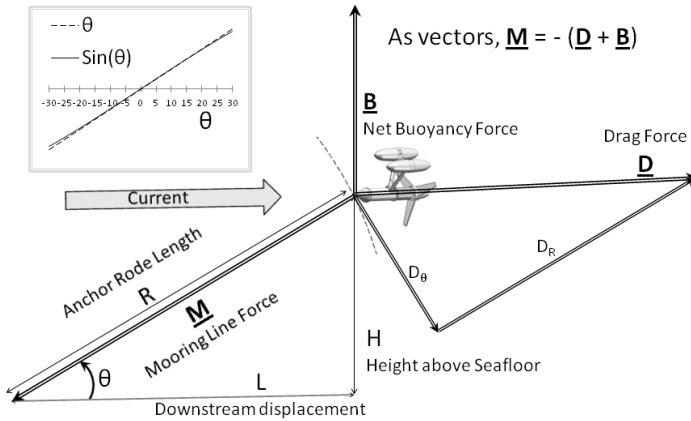


Figure 2: Force diagram of a simple mooring. Current flows from left to right.

use the common notation $\frac{d[\cdot]}{dt} = [\dot{\cdot}]$, with two overdots for the second derivative, (ii) assume that the OCT has mass m , and (iii) neglect friction.

The reference frame of the OCT's mooring is properly formulated in polar coordinates, with the origin at the anchor. The two coordinates are the angle of the rode, θ , and the radial distance along the rode. Projecting the drag force \mathbf{D} onto these coordinates yields the two components D_θ and D_R shown in Fig. 2. As \mathbf{D} varies with current speed, variations in D_R change the magnitude of \mathbf{M} accordingly, while variations in D_θ induce a rotation about the anchor, changing θ . If ω is the rotation rate about the anchor, the appropriate expression of Newton's Second Law here is

$$m \cdot R \cdot \dot{\omega} = m \cdot R \cdot \ddot{\theta} = D_\theta = |\mathbf{D}| \cdot \sin(\theta) \quad (12)$$

In order to analyze the effects of vertical shear, we set the perturbation drag $D_\theta' = |\mathbf{D}'| \cdot \sin(\theta_o) = \gamma \cdot H' \cdot \sin(\theta_o) = \gamma \cdot (H_o/R) \cdot H'$ and note that changes in $H' = R \cdot \sin(\theta')$. Finally, as shown in the upper-left inset in Fig.16 as a reminder, for small angles $\sin(\theta) \approx \theta$. Putting this all together gives

$$\ddot{\theta}' + \frac{\gamma}{mS_o} \theta' = 0, \quad (13)$$

where $S_o = R/H_o$ is the base-state scope of the rode.

Solutions to (13) take the form $\theta' = \theta_1 [\exp(i\omega t) + \exp(-i\omega t)]$, with θ_1 an arbitrary constant. The characteristic equation for this yields

$$\omega = \begin{cases} \varphi & \text{if } \gamma > 0 \\ i\varphi & \text{if } \gamma < 0 \end{cases}, \quad \text{where } \varphi \equiv \sqrt{\frac{|\gamma|}{mS_o}} > 0. \quad (14)$$

Figure 2 also shows the associated mooring geometry, in which the catenary of the mooring rode is ignored, a simplification that does not affect the analysis here. In steady state, it is clear that the scope of the rode is R/H and that this also equals M/B (expressed as magnitudes).

A linear perturbation analysis of this system takes the various quantities to be the sum of a steady base state $[\cdot]_o$ and a small, time-dependent perturbation $[\cdot]'$. We (i)

For cases in which the current speed, and therefore D_{θ}' , increase with height above the bottom (current is faster near the surface), then, small perturbations will lead to a free oscillation whose frequency depends on the base-state geometry, the mass of the OCT, and the strength of this positive shear. Of course, in the real ocean, this free oscillation would be damped by the frictional forces that are ignored here.

Cases of negative shear, $\gamma < 0$, in which the current speed decreases with height above the bottom (or, equivalently, increases with increasing depth from the surface), are of more interest. Here, the solution no longer oscillates:

$$\theta' = \theta_1 \cdot [\exp(-\varphi t) + \exp(\varphi t)] \quad \text{if } \gamma < 0. \quad (15)$$

The first term is of no concern, but the second term shows clearly that in cases of negative vertical shear, small depth perturbations will grow exponentially. Thus, in the absence of additional controls, negative shear is inherently unstable for moored OCTs.

It is worth re-emphasizing that this results depends on the assumption that the net buoyancy **B** is constant. It may therefore be possible to control this instability with variable (net) buoyancy, which control process could involve variable lift from the OCT control surfaces.

The physical basis for the instability can be stated in simple terms, because (for the assumptions here) flow perturbations affect the drag while the net buoyancy remains constant. Relative to a balanced base state, a slow-flow perturbation will create an imbalance of (positive) buoyancy, causing the OCT to rise; a fast-flow perturbation will create an imbalance of extra drag and therefore a buoyancy deficit relative to the base-state balance, causing the OCT to dive. If the OCT rises or dives into faster or slower water, respectively, then the imbalances will tend to be corrected. On the other hand, if the slow-flow, rising imbalance puts the OCT into even slower water, the imbalance will be amplified, as it will for the fast-flow imbalance that dives the OCT into faster water. In other words, the configuration of the rode is such that it pulls the OCT toward water of the same sense as the initial perturbation in the unstable case.

Note that the strength of the instability—the magnitude of the time constant φ —depends inversely on the base-state scope of the mooring: longer scope moorings, with longer time constants, are less sensitive to perturbations and therefore more amenable to control processes. Of course, these moorings are also more expensive due to the cost of the rode.

In the context of this discussion of instability associated with vertical shear in the current, it is appropriate to include a qualitative look at two secondary effects on bottom-moored OCTs when one of the assumptions here is relaxed. These effects cannot be quantified without a dynamic model of a specific OCT and its mooring, but there are certain qualitative aspects of design that factor in to the stability issue.

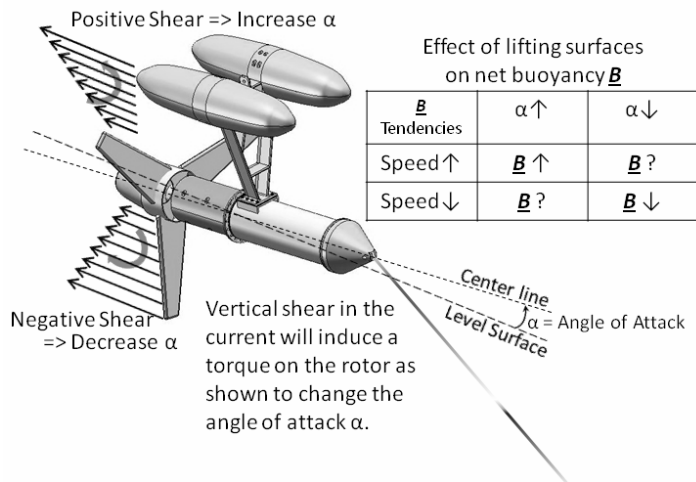


Figure 3: Effects of vertical shear on lift.

discussion of vertical shear.

Consider first the effects of vertical shear on angle of attack (Fig. 3). Below the lifting-surface stall limit, increases in angle of attack will tend to increase lift. To the extent that there is a cross-rotor torque introduced by vertical shear, the angle of attack becomes part of the overall effect of shear. For both leading-rotor systems and trailing-rotor systems, positive shear would tend to induce nose-up pitch, increasing the angle of attack; the opposite would happen with negative shear. Positive vertical shear, then, increases lift and negative vertical shear decreases lift. The latter would tend to exacerbate the instability associated with negative vertical shear discussed above.

The effects on lift of current speed are also relevant. In general, increased speed will increase lift (again, assuming that the system's angle of attack is below the stall limit). In the case of positive vertical shear, the overall effect here will be the same as that for the changes of angle of attack. In the case of negative vertical shear, however, they will be the opposite, tending to counterbalance the exacerbation of the fundamental instability. Quantifying the net effect of these two components of lift is not possible without a detailed model of the system under consideration. This result, however, argues for active lifting surfaces so that these effects can be controlled.

Note that, in Fig. 2, the basic force balance of the system under consideration includes a *net* buoyancy force \underline{B} (which, although a vector, can be assumed to have only a vertical component). This net buoyancy force is the sum of the buoyancy and whatever lift the design of the OCT generates; the previous results depend on the assumption that \underline{B} is constant. In reality, the lift is likely to be dependent on both current speed and the OCT's angle of attack. Both of these dependencies factor in to the